

OPEN ACCESS

Evaluation of Options and Limits of Aqueous All-Quinone-Based Organic Redox Flow Batteries

To cite this article: Stina Bauer *et al* 2020 *J. Electrochem. Soc.* **167** 110522

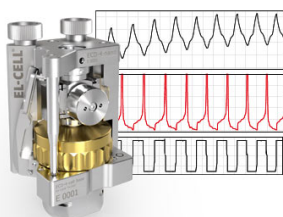
View the [article online](#) for updates and enhancements.

You may also like

- [A Mathematical Physicist's Approach to Virology](#)
Reidun Twarock
- [Lithium-Silicon Compounds as Electrode Material for Lithium-Ion Batteries](#)
Daniel Uxa, Erwin Hüger, Lars Dörrer et al.
- [Highly carbide filled composite materials for the mining and drilling industry](#)
Ch Gerck, L Yan-Gerk, V Wesling et al.

Measure the Electrode Expansion in the Nanometer Range. Discover the new ECD-4-nano!

EL-CELL[®]
electrochemical test equipment



- Battery Test Cell for Dilatometric Analysis (Expansion of Electrodes)
- Capacitive Displacement Sensor (Range 250 μm , Resolution ≤ 5 nm)
- Detect Thickness Changes of the Individual Electrode or the Full Cell.

www.el-cell.com +49 40 79012-734 sales@el-cell.com





Evaluation of Options and Limits of Aqueous All-Quinone-Based Organic Redox Flow Batteries

Stina Bauer,^{1,2,3,z}  Jan C. Namyslo,¹ Dieter E. Kaufmann,¹  and Thomas Turek^{2,3} 

¹Institute of Organic Chemistry, Clausthal University of Technology, 38678 Clausthal-Zellerfeld, Germany

²Institute of Chemical and Electrochemical Process Engineering, Clausthal University of Technology, 38678 Clausthal-Zellerfeld, Germany

³Research Center Energy Storage Technologies (EST), 38640 Goslar, Germany

Redox flow batteries based on aqueous electrolytes with organic active material (ORFB) have great potential for the development of environmentally safe and ecologically sustainable energy storage systems. To be competitive with the state-of-the-art vanadium redox flow battery, organic electrolytes must meet a whole range of requirements. We investigated different anthraquinone-based electrolytes, i.e. anthraquinone-2,6-disulfonic acid, anthraquinone-2,7-disulfonic acid (2,7-AQDS), anthraquinone-2-sulfonic acid, and 1,2-dihydroxybenzene-3,5-disulfonic acid (BQDS) with respect to their solubility in sulfuric acid, their electrical conductivity, and their viscosity. For this purpose, the influence of the concentration of sulfuric acid and the active species on the electrolyte properties was determined. Using NMR spectroscopy we analysed the thermal and electrochemical stability of 2,7-AQDS and BQDS electrolytes. The electrochemical stability was also monitored by cyclic voltammetry. Both methods have also indicated the absence of crossover phenomena. Furthermore, the influence of the electrolyte properties on the performance of the ORFB was investigated. Comparison with the vanadium electrolyte allowed us to estimate these kinds of requirements in order to develop a comparable all-organic flow battery.

© 2020 The Author(s). Published on behalf of The Electrochemical Society by IOP Publishing Limited. This is an open access article distributed under the terms of the Creative Commons Attribution Non-Commercial No Derivatives 4.0 License (CC BY-NC-ND, <http://creativecommons.org/licenses/by-nc-nd/4.0/>), which permits non-commercial reuse, distribution, and reproduction in any medium, provided the original work is not changed in any way and is properly cited. For permission for commercial reuse, please email: permissions@iopublishing.org. [DOI: [10.1149/1945-7111/aba338](https://doi.org/10.1149/1945-7111/aba338)]



Manuscript submitted December 20, 2019; revised manuscript received June 4, 2020. Published July 13, 2020.

Continuously, the public has become more and more aware of a man-made climate change. To reduce greenhouse gas emissions, the basis for the generation of electricity has to be changed from fossil fuels to renewable sources like wind or solar power. At the same time this will increase the demand for efficient and cost-effective energy storage systems that are able to buffer the fluctuation between energy production and consumption in order to maintain a stable electricity grid.^{1,2}

Redox flow batteries (RFBs) represent a promising storage technology for stationary applications. Characteristics of RFBs are the decoupled parts responsible for capacity (volume of tanks) and power (area of cells) as well as the presence of flowable electrolytes containing a redox active species.³⁻⁹

The most widely studied redox active species soluble in aqueous solutions are vanadium salts, the first application of which in a RFB was described by Rychcik and Skyllas-Kazacos.¹⁰ Vanadium possesses four different stable oxidation states to form two redox couples ($\text{VO}_2^+/\text{VO}^{2+}$ and $\text{V}^{2+}/\text{V}^{3+}$), which are stable in strong acids such as sulfuric acid. Their redox potentials differ to an extent that an open-circuit voltage of approximately 1.3 V can be achieved.¹¹ The advantages of an all-vanadium redox flow battery (VRFB) include long cycle stability, high energy efficiency, avoiding cross-contamination and low self-discharge.^{12,13} Main disadvantages include the corrosive and toxic properties of the vanadium electrolytes,¹² the small temperature window of 5 °C to 40 °C, in which the VRFB can be operated without precipitation of an insoluble vanadium salt,¹³ the high costs for material and periphery,¹⁴ and the limited availability of vanadium resources.¹⁵

In 2014, Aziz and co-workers demonstrated the applicability of electrolytes based on organic molecules in a RFB.¹⁶ Since then, research in the synthesis of new organic redox active species soluble in aqueous or non-aqueous solvents has been intensified.^{3,17-19} The use of organic molecules as redox active pairs has several advantages. They are potentially low cost materials, naturally occurring without scarcity, when they are obtained from renewable raw materials via industrial biotechnology or through power-to-X technologies.^{3,4} Due to a fundamental adaptability of organic molecules, it is possible to adjust properties such as solubility,

chemical/electrochemical stability or redox potential by functionalization of the active key structure via simple and economic syntheses.^{20,21} The organic species are also expected to be less toxic and corrosive, which would allow access to environmentally safe and ecologically sustainable RFBs.³

In the field of RFBs based on aqueous electrolytes with organic active material (ORFB), quinones have proven to be particularly suitable because they are capable of fast and reversible proton-coupled 2-electron transfer reactions.^{22,23} In some reports, these quinones were combined with inorganic redox active materials such as transition metal halides^{16,24-28} or hexacyanidoferrate (III)²⁹⁻³⁶ to build up the battery. In other studies, quinones with clearly different potentials were used both in the positive and negative half cell of the ORFB.³⁷⁻⁴⁴ Since only one electron per redox couple can be exchanged simultaneously in most metal-based RFBs, very different concentrations of all components (active species, supporting electrolyte, etc.) are required in both half cells of an organic-inorganic RFB. In an ORFB based only on quinones, the same conditions can be used in the entire cell. We think that this is an enormous advantage of a completely organic RFB in terms of crossover effects, atomic economy and contributes to cost reduction.

Since the V(V) electrolyte is susceptible to precipitation at permanent temperatures above 40 °C, VRFB cannot be operated at this temperature.⁴⁵⁻⁴⁷ For the ORFB, it would be advantageous if the organic electrolytes are stable at these and even higher temperatures, which also could improve the solubility and increase the reaction rate.

Therefore, we determined major parameters such as solubility in sulfuric acid, electrical conductivity and viscosity of different anthraquinone-based electrolytes, i.e. anthraquinone-2,6-disulfonic acid (2,6-AQDS), anthraquinone-2,7-disulfonic acid (2,7-AQDS), anthraquinone-2-sulfonic acid (2-AQS), and 1,2-dihydroxybenzene-3,5-disulfonic acid (BQDS) based electrolytes to overview the electrolyte properties in a comprehensive and comparative manner. Furthermore, we analysed the thermal stability of 2,7-AQDS and BQDS electrolyte by nuclear magnetic resonance (NMR) spectroscopy after prolonged storage at 40 °C. In addition to the thermal stability, we also considered the electrochemical stability of 2,7-AQDS and BQDS electrolytes after charge/discharge studies in a flow cell by using NMR spectroscopy and cyclic voltammetry (CV). Comparison of all these information with those of the vanadium electrolytes permits us to

^zE-mail: stina.bauer@tu-clausthal.de

formulate requirements for organic electrolytes in order to develop a comparable all-organic RFB.

Experimental

Substances.—Anthraquinone-2,7-disulfonic acid (2,7-AQDS) disodium salt was purchased from TCI chemicals (>97%) and aber GmbH (80%), 1,2-dihydroxybenzene-3,5-disulfonic acid (BQDS) disodium salt monohydrate (>98%) from TCI chemicals, anthraquinone-2,6-disulfonic acid (2,6-AQDS) disodium salt (>90%) from acros organics and anthraquinone-2-sulfonic acid (2-AQS) sodium salt monohydrate (>97%) from Sigma-Aldrich. All these salts were used as received. According to the literature the sodium salt was dissolved in deionized water and flushed twice through a column containing Amberlyst® 15 hydrogen form ion exchange resin purchased from Sigma-Aldrich and activated with hydrochloric acid to prepare the acid form.¹⁶ The vanadium electrolyte (1.6 M total vanadium and 4 M sulfuric acid) was purchased from GFE (Gesellschaft für Elektrometallurgie mbH, Nürnberg, Germany) and charged, respectively discharged to receive the vanadium species in all four oxidation states.

Solubility.—The solubility of quinones at room temperature and 40 °C was measured in deionized water (18.2 MΩ cm, Merck Millipore, USA) and 1, 2, 3, and 4 M sulfuric acid (98%, Sigma-Aldrich) prepared from deionized water both for the sodium salt and the acid form. To ascertain the solubility limit a defined amount of quinones was first weighed out. Then each solvent was gradually added until no further solid could be dissolved. Based on both amounts the solubility was calculated. This procedure was executed three times and the arithmetic average of the calculated solubility was determined.

Electrical conductivity.—Quinones were dissolved in 1, 2, 3 and 4 M sulfuric acid to prepare a concentration series according to the solubility. Stirring constantly, the temperature of quinone containing electrolytes was stabilized at 25 °C. The conductivities were determined with a SevenGo Duo pH/Ion/Cond meter SG78-FK2-K from Mettler-Toledo (Gießen, Germany). Again, the measurements were executed three times and the arithmetic average of the conductivity was calculated. In the same way, the conductivity was determined for the vanadium electrolyte in the charged and discharged state, respectively.

Viscosity.—To ascertain the viscosity of the quinone and the vanadium electrolytes, the temperature of the Ubbelohde viscometer 50101/Oa of SI Analytics with a device-specific constant K of 0.005 was stabilized at 25 °C. Again, the measurements were executed three times and the arithmetic average of the kinematic viscosity was estimated. Therefore, a correction according to Hagenbach-Couette was taken into account. Using the density the dynamic viscosity was calculated.

Thermal stability analysis at 40 °C by proton NMR spectroscopy.—Electrolyte solutions of BQDS and 2,7-AQDS were prepared each in acid form with a concentration of 0.1, 0.5 and 1.0 M. In all cases, 1 M sulfuric acid was used as supporting electrolyte. The temperature of the samples was stabilized at 40 °C and stored for 6 months. The molecular structure of the electrolytes was analysed by NMR spectroscopy using a Bruker Digital FT-NMR spectrometer Avance III 600 MHz before and after storage. For this purpose, 90 μL of the electrolyte were diluted with 450 μL deuterated water (D₂O) containing trimethylsilylpropanoic acid (TMSP) as internal reference. The chemical shifts were determined relative to the TMSP signal (0.00 ppm).

Charge/discharge studies in a flow cell.—For the charge/discharge studies, a flow-through cell with a symmetrical setup on the positive and the negative side was employed. To separate the half

cells, a Nafion™ N117 proton-exchange membrane was used. The membrane was sandwiched between the carbon felt electrodes (Sigracell® GFD 2.5 EA, SGL Carbon SE, Germany) with an active electrode area of 10 cm² and a compression rate of 15%. To position the electrodes, they were inserted into an acrylic glass frame (thickness 1.1 mm, Formulor GmbH, Germany) covered by silicone rubber seals (thickness 1.0 mm, Formulor GmbH, Germany). Through the inner area of the frame and the seal, the electrodes were in contact with graphite bipolar plates (PPG 86, Eisenhuth GmbH & Co. KG, Germany). The plates were covered by gold-plated nickel meshes, which were connected at the upper end with copper plates. This arrangement acted as a current collector and was protected from direct contact with the electrolytes by the graphite bipolar plates. For electrical insulation, each side was closed with a polymethylmethacrylate plate. Using six bolts and nuts, the cell was tightened to a torque of 1.0 N for each bolt. All charge/discharge studies were carried out with BQDS as positive electrolyte and 2,7-AQDS as negative electrolyte, each in acid form. 1.0 M sulfuric acid was used as supporting electrolyte. The electrolyte volume was 90 mL. Samples with a quinone concentration of 0.1 and 0.5 M were investigated, with the same concentration always being used in each half cell. Two glass containers were used to store the solutions at all times during the studies under a constant humid nitrogen flow in order to avoid oxidation. To circulate the electrolytes through the cell, we utilized membrane liquid pumps from KNF (NF 1.25 RTDC) with a flow rate of 46 mL min⁻¹ for each half cell.

The cutoff voltage for charge/discharge studies was set to 1.000 V for charging and to 0.005 V for discharging. All 30 charge/discharge cycles were performed at room temperature under constant current density of 80 mA cm⁻² using a battery test system from BaSyTec GmbH (782 XCTS, 12 Channel, 25 A). After the first and the last cycle, a polarization curve was taken at multiple discharge current steps in the range from 0 to 200 mA cm⁻².

Electrochemical stability analysis of electrolyte after charge/discharge studies.—In order to quantify the electrochemical stability of quinone electrolytes, they were examined before and after charge/discharge studies in the flow cell using cyclic voltammetry (CV) and NMR spectroscopy. For the NMR analysis, the same conditions as described above were used. For the CV analysis, 10 mL of the electrolyte were filled in a four-neck flask containing a static glassy carbon rotating disk electrode (active area 0.2 cm², Princeton Applied Research, USA) as working electrode, a platinum mesh as counter electrode, and a reversible hydrogen reference electrode (RHE, Hydroflex®, Gaskatel, Germany) as reference electrode arranged in a three electrode set-up. All electrodes were connected to a Biologic SP-50 potentiostat to carry out the measurements at a scan rate of 25 mV s⁻¹ over a potential range of -0.3 respectively -0.2 to 1.2 V vs RHE.

Results and Discussion

Solubility of the acid form and the sodium salt of quinones.—The solubility of 2,7-AQDS, 2,6-AQDS, 2-AQS, and BQDS both in the acid form and as sodium salt in sulfuric acid with different concentrations measured under comparable conditions at 20 °C and 40 °C is depicted in Fig. 1 and Table I. Deionized water was used as solvent, indicated as sulfuric acid with a concentration of 0 M. The solubility of 2-AQS both in the acid form and as sodium salt is very low in all concentrations of sulfuric acid compared to the other quinones. In case of 2,6-AQDS, the acid form is more soluble than the sodium salt at all concentrations of sulfuric acid. This is consistent with the observation made by Yang et al.⁴¹

The acid forms of 2,7-AQDS and BQDS are also better soluble than the sodium salts. Furthermore, the solubility of both substances decreases with increasing sulfuric acid concentration and with decreasing pH, respectively. This effect is observed both at 20 °C and 40 °C. In addition, the solubilities of 2,7-AQDS are all in all higher than those of BQDS. Thus, the concentration of BQDS would

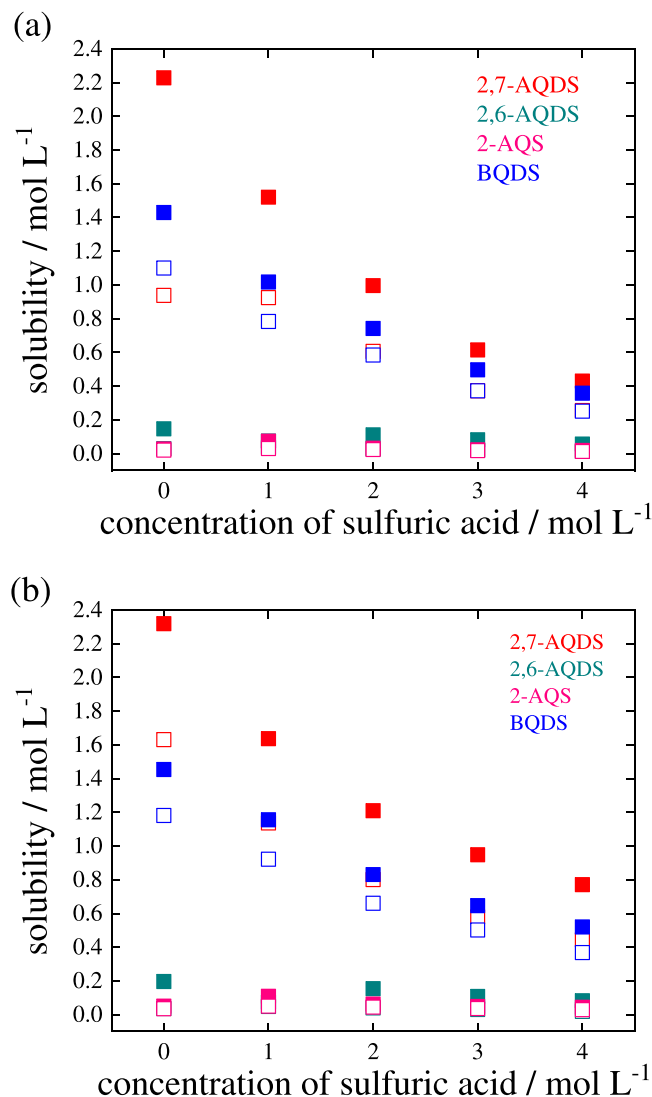


Figure 1. Solubility of 2,7-AQDS, 2,6-AQDS, 2-AQS, and BQDS as acid (■) and sodium salt (□) as function of the sulfuric acid concentration at 20 °C (a) and 40 °C (b).

be the limiting parameter by realizing an all-quinone RFB. As expected, the overall solubility is better at 40 °C than at 20 °C. Increase of the operating temperature range could therefore lead to a higher energy density of the ORFB.

In VRFB, the solubility of the vanadium species also depends on the concentration of sulfuric acid and temperature.^{45,48–50} Although

more than 2 M of V can be dissolved in sulfuric acid, stability studies of Skyllas-Kazacos and co-workers have shown that a concentration around 1.5 M V in 3–4 M sulfuric acid is most suitable for cycling conditions up to temperatures of 40 °C.⁴⁵ Since the quinones are capable of exchanging twice as many electrons per redox couple as vanadium, it would be sufficient if their solubility is half the solubility of the vanadium species (~0.7 M) to achieve comparable energy densities.

According to this, the solubilities of 2-AQS and 2,6-AQDS both in acid form and as sodium salt are far too low to be suitable for the application in an ORFB. In contrast, BQDS and 2,7-AQDS dissolve much better in sulfuric acid. Though, the solubilities of BQDS and of 2,7-AQDS in 3 M and 4 M sulfuric acid are still below the limit of 0.7 M and are therefore also unsuitable (sole exception: acid form of 2,7-AQDS at 40 °C). If 2 M sulfuric acid is used as solvent, the solubilities of the sodium salts of BQDS and 2,7-AQDS are below the limit, whereas that of the acid forms are above the limit. In case of 1 M sulfuric acid, however, the solubilities are significantly higher and the acid forms are even in the range of the vanadium species. This sulfuric acid concentration appears to be particularly suitable for an ORFB. Moreover, conversion of the sodium salt into the acid form is also worthwhile since the solubility can be significantly increased.

Electrical conductivity and viscosity studies.—The electrical conductivity of various concentrated solutions using BQDS and 2,7-AQDS both in the acid form with 1 M and 4 M sulfuric acid as solvents (Fig. 2a) was also investigated. For better comparison, the conductivities of the vanadium electrolytes were also measured. It is obvious that the conductivity decreases with an increasing concentration of the active organic species. As expected, the highest conductivity of sulfuric acid is observed at a concentration of 4 M,⁵¹ but it is noticeable that the conductivity of 4 M sulfuric acid decreases significantly more rapidly with an increasing quinone concentration than with 1 M sulfuric acid as solvent. Apparently, the interaction between sulfuric acid and quinone molecules gets stronger in case of higher concentrations. As a consequence, the self-dissociation of the sulfuric acid molecules is hindered and thus the electrical conductivity massively decreases. At higher quinone concentrations, the conductivities of the 2,7-AQDS containing solutions are lower than those of the BQDS solutions. In addition to the interaction with the sulfuric acid molecules, 2,7-AQDS is also self-interacting, leading to a further reduction of the conductivity. If 1 M sulfuric acid is used as solvent, the amount of sulfuric acid molecules is significantly lower. Here the self-dissociation of the sulfuric acid molecules is hindered, only at a much higher concentration of quinones. Furthermore, only slight differences in conductivity of BQDS and 2,7-AQDS were found which means, that using 1 M sulfuric acid the amount of molecules has a stronger influence on the conductivity than the chemical structure.

Additionally, the conductivity of the 4 M sulfuric acid is also distinctly reduced in case of vanadium ions as active species. Even

Table I. Solubility of 2,7-AQDS, 2,6-AQDS, 2-AQS, and BQDS as acid and sodium salt in different sulfuric acid concentrations at 20 °C and 40 °C.

	Solubility/mol L ⁻¹									
	0 M H ₂ SO ₄		1 M H ₂ SO ₄		2 M H ₂ SO ₄		3 M H ₂ SO ₄		4 M H ₂ SO ₄	
	20 °C	40 °C	20 °C	40 °C	20 °C	40 °C	20 °C	40 °C	20 °C	40 °C
2,7-AQDS	2,23	2,32	1,52	1,64	1,00	1,21	0,61	0,95	0,43	0,77
2,7-AQDS-Na ₂	0,94	1,63	0,92	1,14	0,61	0,80	0,37	0,58	0,26	0,44
2,6-AQDS	0,15	0,20	0,08	0,07	0,11	0,15	0,08	0,11	0,06	0,08
2,6-AQDS-Na ₂	0,03	0,04	0,04	0,05	0,03	0,04	0,02	0,03	0,01	0,02
2-AQS	0,03	0,05	0,07	0,11	0,03	0,06	0,02	0,05	0,02	0,04
2-AQS-Na	0,02	0,04	0,03	0,05	0,02	0,04	0,02	0,04	0,01	0,03
BQDS	1,43	1,45	1,02	1,16	0,74	0,83	0,50	0,65	0,36	0,52
BQDS-Na ₂	1,10	1,18	0,78	0,92	0,58	0,66	0,37	0,50	0,25	0,37

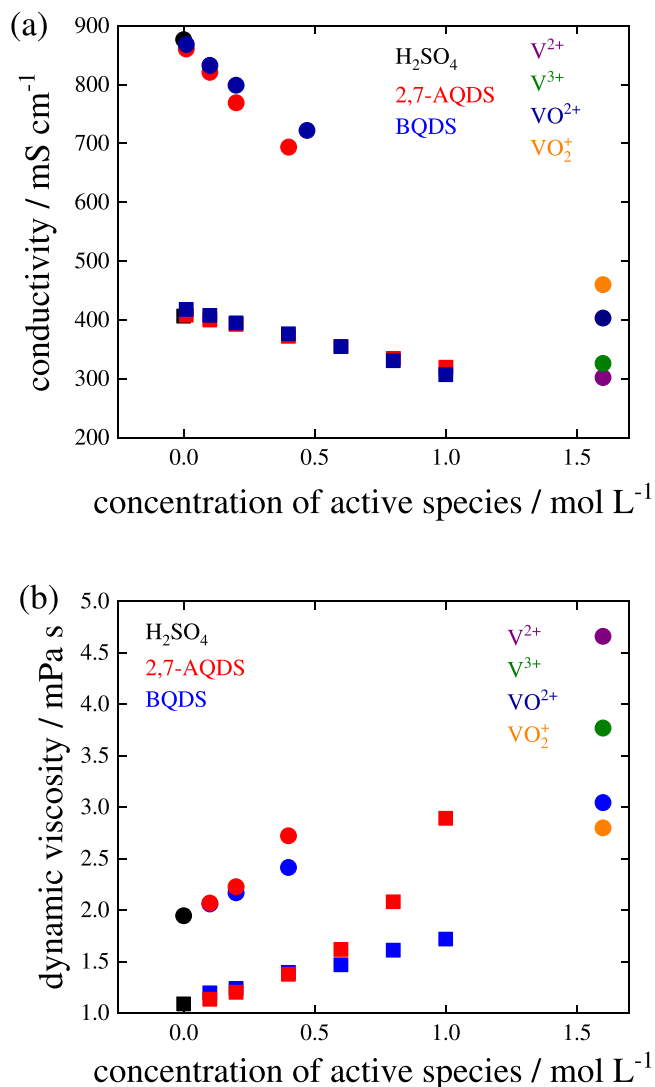


Figure 2. Conductivity (a) and dynamic viscosity (b) of 2,7-AQDS, BQDS, VO₂⁺, VO²⁺, V²⁺, and V³⁺ dissolved in 1 M (■) and 4 M H₂SO₄ (●) measured at 25 °C as function of the concentration of active species.

the conductivities of the individual vanadium species differ significantly, which has also been reported by Skyllas-Kazacos and co-workers.⁴⁵ Our own studies also show that the conductivities of all solutions with quinones as the active species and with 1 M sulfuric acid as solvent are in the range of the vanadium electrolytes

using 4 M sulfuric acid as supporting electrolyte. This means that although the intrinsic conductivity of 1 M sulfuric acid is significantly lower than the one of 4 M sulfuric acid, the 1 M sulfuric acid is suitable for realizing quinone electrolytes comparable to the vanadium electrolytes, since the molecular influences on 4 M sulfuric acid as supporting electrolyte are significantly higher than on lower sulfuric acid concentrations.

Figure 2b shows the results of the viscosity studies with 1 M and 4 M sulfuric acid as supporting electrolyte. For this, we used the same solutions as for the conductivity studies. It is obvious that with increasing quinone concentration the viscosity of the solution increases considerably. By using 4 M sulfuric acid as the solvent, the viscosities of the solutions are overall significantly higher than of those using 1 M sulfuric acid. Furthermore, the viscosities of the solutions with BQDS or 2,7-AQDS as active species do not differ up to a quinone concentration of 0.4 M (1 M sulfuric acid) and 0.2 M (4 M sulfuric acid), respectively. At low concentration of active species, the increase in viscosity originates mainly from the interactions between sulfuric acid and the quinone. At higher concentrations, the viscosity of the solutions containing 2,7-AQDS increases considerably stronger than the one of the BQDS solution. We assume that starting at a concentration 0.6 M (1 M sulfuric acid) and 0.4 M (4 M sulfuric acid), respectively, the 2,7-AQDS molecules interact more strongly with each other. In addition to the interactions between the sulfuric acid and 2,7-AQDS molecules, also π - π -interactions between the aromatic rings of two 2,7-AQDS molecules occur, resulting in much more viscous solutions. In contrast, BQDS molecules are not known for π - π -interactions. Here, the viscosity increase is still based on the increasing interactions due to the rising overall concentration.

In order to clearly classify the results of the viscosity studies, the respective values for the vanadium electrolytes were also determined (Fig. 2b). The viscosities of the individual vanadium species differ distinctly, which is in agreement with literature data.^{49,52} Overall, the vanadium containing solutions are clearly more viscous than the quinone containing ones, regardless whether 1 M or 4 M sulfuric acid is used as a solvent.

In this case, an ORFB would have an advantage over VRFB. Due to the lower viscosity, the quinone electrolytes are easier to pump, which reduces the pressure drop along the cells and the corresponding pumping costs.

Analysis of thermal stability by proton NMR spectroscopy.—

Figure 3a shows the ¹H-NMR spectra of three differently concentrated solutions with 2,7-AQDS as active species before storage at 40 °C. 2,7-AQDS possesses 6 aromatic protons. As a result of the molecular symmetry, two of these protons have an identical magnetic environment, are therefore equivalent and lead to the same chemical shifts in NMR. The spin-spin-coupling of the non-isochronous protons with each other leads to the splitting of signals. With the help of the resulting

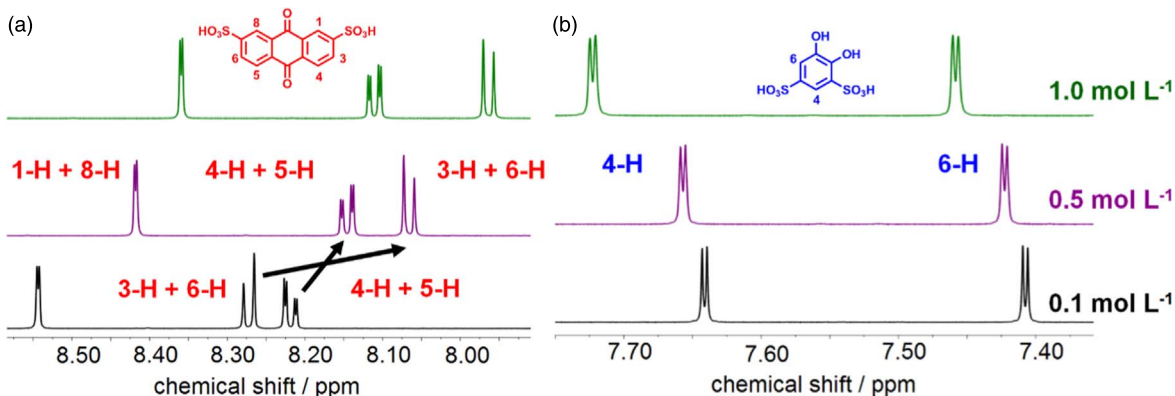


Figure 3. ¹H-NMR spectra at 600 MHz of 2,7-AQDS (a) and BQDS (b) both dissolved in 1 M H₂SO₄ with a quinone concentration of 0.1 M, 0.5 M or 1.0 M before storing at 40 °C. Solutions were diluted with deuterated water (5 D₂O: 1 sample). The chemical shifts were determined relative to the TMSp signal.

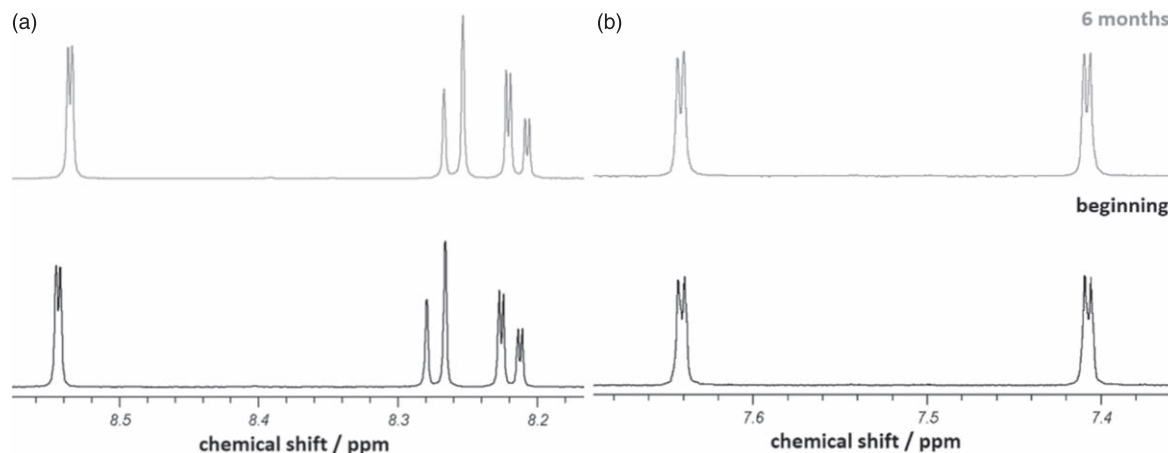


Figure 4. $^1\text{H-NMR}$ spectra at 600 MHz of 2,7-AQDS (a) and BQDS (b) both dissolved in 1 M H_2SO_4 with a quinone concentration of 0.1 M before and after storing 6 months at 40 °C. Solutions were diluted with deuterated water (5 D_2O : 1 sample). The chemical shifts were determined relative to the TMS signal.

coupling constants and by measuring 2D-NMR spectra, the unambiguous assignment of the proton signals is possible. Proton NMR measurement at a 2,7-AQDS concentration of 0.1 M reveals the doublet at 8.54 ppm ($^3J = 1.8$ Hz, 2H) that belongs to the protons in the 1- and 8-position, the doublet at 8.27 ppm ($^3J = 8.1$ Hz, 2H) from the protons in 3- and 6-position, and the doublet of doublets at 8.21 ppm ($^3J = 1.8$ Hz and $^3J = 8.1$ Hz, 2H) from the protons in 4- and 5-position, respectively. The increasing 2,7-AQDS concentration leads to a change in chemical shifts. The protons are shielded more strongly, which can be distinguished by a signal shift to lower ppm values. Furthermore, a change of the signal sequence takes place. In detail, the signals of the protons at 4- and 5-position appear at 8.15 ppm (0.5 M) or at 8.11 ppm (1.0 M) and that of protons in 3- and 6-position at 8.07 ppm (0.5 M) or at 7.96 ppm (1.0 M). Expectedly, the coupling constants do not change. We consider this striking proton signal change to be triggered by increasing π - π -interactions between the aromatic rings of 2,7-AQDS upon increasing substance concentration, resulting in a change of the magnetic environment. The NMR study also confirms the results of the viscosity analysis (Fig. 2b), in which a massive increase of viscosity with rising 2,7-AQDS concentration can likewise be observed.

$^1\text{H-NMR}$ spectra of the three differently concentrated BQDS solutions before storage at 40 °C are shown in Fig. 3b. In contrast to 2,7-AQDS, BQDS comprises only two non-isochronous protons. At a BQDS concentration of 0.1 M, the resulting doublet at 7.64 ppm ($^3J = 2.2$ Hz, 1H) can be assigned to the proton in 4-position and the doublet at 7.41 ppm ($^3J = 2.2$ Hz, 1H) to 6-position. A signal alteration as seen above with increasing BQDS concentration does not occur. Only a small signal shift to higher ppm values is found, which means that the particular protons are deshielded with increasing concentration. The detection of the protons of the sulfonic acid groups is not possible in both cases, since these coincide with the signals of the water due to chemical exchange.

After a storage period of 6 months at 40 °C, the samples were reviewed. Optically, there were no changes visible as neither the color changed nor precipitation had taken place. The NMR spectroscopic analysis also revealed that the solutions are stable over this period, since the $^1\text{H-NMR}$ spectra before and after storage are consistent in signal position and sequence. In addition, no further signals occurred, which would be an indication of thermal decomposition. As an example, the $^1\text{H-NMR}$ spectra of solutions containing 2,7-AQDS (Fig. 4a) and the BQDS (Fig. 4b) with a concentration of 0.1 M before and after storage at 40 °C are shown in Fig. 4.

Stability analysis of electrolytes after charge/discharge studies in flow cells.—We investigated the electrochemical stability of 2,7-AQDS and BQDS electrolyte by comparing the cyclic voltammograms and the NMR spectra of the electrolytes before and after

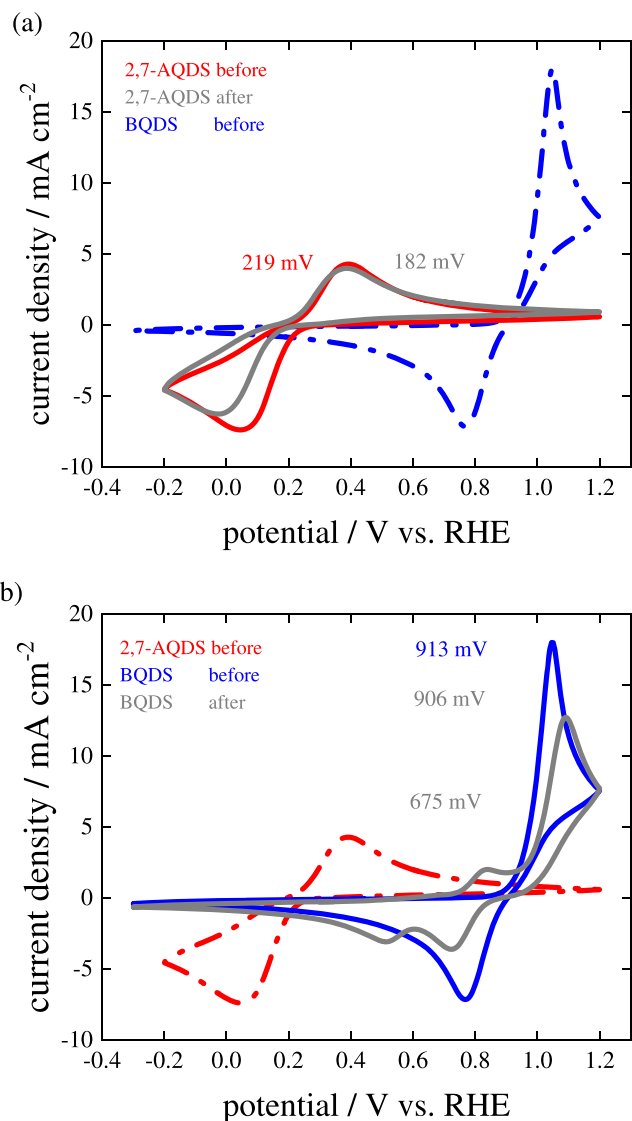


Figure 5. Cyclic voltammograms at 25 mV s^{-1} for 100 mM 2,7-AQDS in 1 M H_2SO_4 before and after charge/discharge studies (a) and for 100 mM BQDS in 1 M H_2SO_4 before and after charge/discharge studies (b). Dashed lines: other electrolyte before charge/discharge studies.

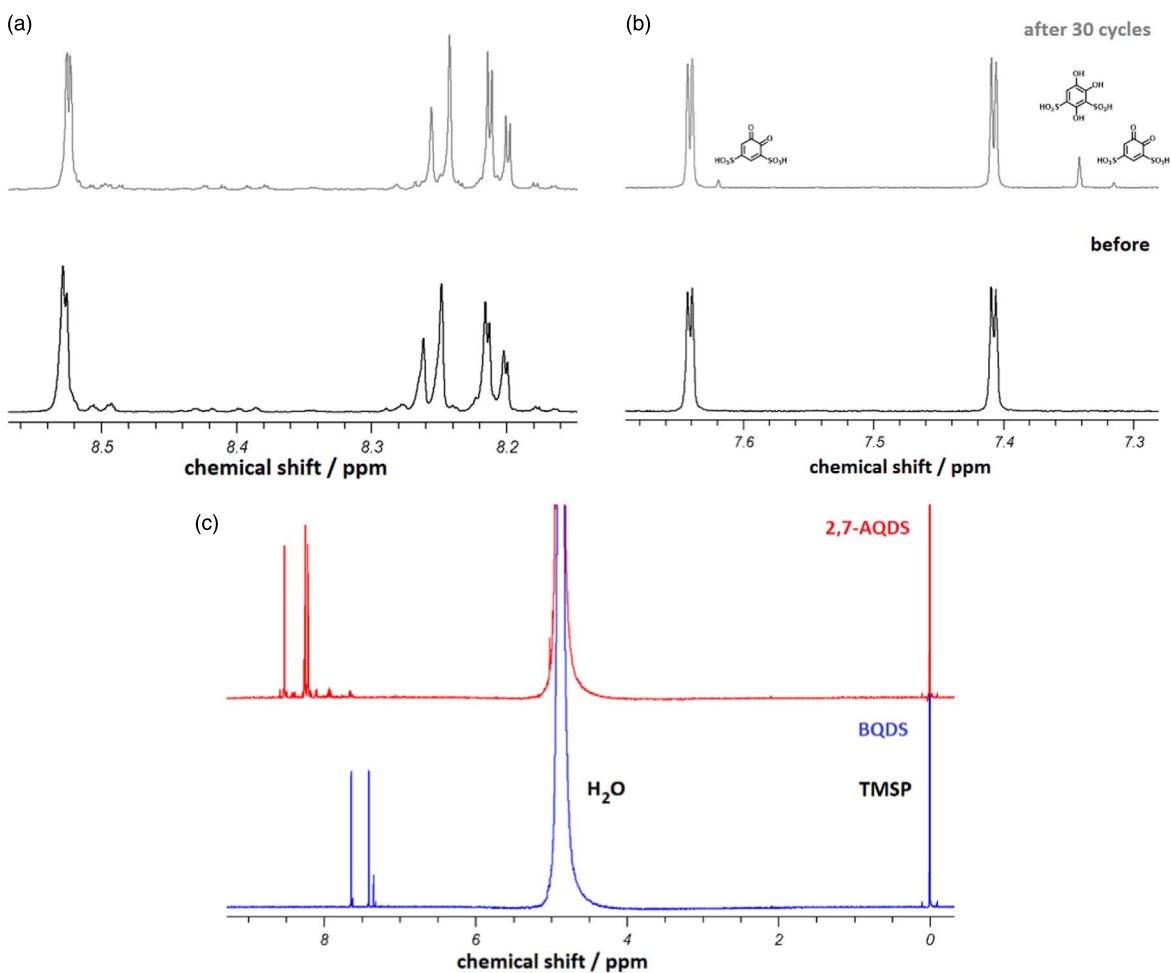


Figure 6. ¹H-NMR spectra at 600 MHz of 2,7-AQDS (a) and BQDS (b) both dissolved in 1 M H₂SO₄ with a quinone concentration of 0.1 M before and after the charge/discharge studies. (c) Entire ¹H-NMR spectra at 600 MHz of 2,7-AQDS and BQDS. Solutions were diluted with deuterated water (5 D₂O: 1 sample). The chemical shifts were determined relative to the TMS signal.

charge/discharge studies in flow cell, respectively. The advantage of analysing electrolytes with cyclic voltammetry compared to NMR analysis is that the electrolytes can be used as received. A change of conditions due to the addition of supplementary substances during necessary NMR sample preparation could be avoided.

Figure 5 shows the cyclic voltammograms of the 2,7-AQDS electrolyte (Fig. 5a) and the BQDS electrolyte (Fig. 5b) before and after cycling. Before cycling, the 2,7-AQDS electrolyte has one peak each in the cathodic and anodic domain at a low potential range, which means that 2,7-AQDS solved in 1 M sulfuric acid undergoes a reversible 2-electron transfer reaction. After cycling, the peak of the reduction reaction of the 2,7-AQDS electrolyte is shifted to a slightly lower potential. Apart from that, the CV data of the 2,7-AQDS electrolyte do not differ. Nevertheless, it has the consequence that the redox potential decreases from 219 mV vs. RHE to 182 mV vs. RHE. The CV data of the BQDS electrolyte before cycling is also shown in Fig. 5a. It turns out, that neither before nor after the charge/discharge studies there are any peaks in the cyclic voltammograms of the 2,7-AQDS electrolyte in the range of the BQDS peaks. This is an indication that there has been no crossover of the BQDS. If this had been the case, peaks in the high potential range would have occurred after cycling. Therefore, the CV measurement can also be used to determine crossover phenomena. As a consequence, the 2,7-AQDS electrolyte has not changed and can be regarded as stable, both thermally and electrochemically.

On the other hand, the CV data of the BQDS electrolyte before and after the charge/discharge studies differ from each other (Fig. 5b). Before cycling, the BQDS electrolyte also undergoes a

reversible 2-electron transfer reaction resulting in one peak each in the cathodic and anodic domain at the high potential range. After cycling, a new peak can be recognized each in both domains, which is potentially a result of the occurring Michael reaction, which would be in agreement with literature.^{39,41,53–55} Furthermore, it can be determined that one new species has formed, which is also redox active and also undergoes a reversible 2-electron transfer reaction. However, the redox potential of this compound is lower (675 mV vs. RHE) than that of BQDS (906 mV vs. RHE). Using CV, it is therefore possible to comprehend the changes of the BQDS electrolyte, but it is not possible to gain structural information about the new compound. For this purpose, a method for structure determination like NMR spectroscopy is required. The CV data of the 2,7-AQDS electrolyte before cycling is shown in Fig. 5b. Since there is no agreement between the peaks of 2,7-AQDS and those of BQDS and the possible Michael product, it can also be assumed that no crossover took place.

The NMR spectroscopical analysis of the electrolytes confirms the results of the CV examination. No further signals can be detected in the ¹H-NMR spectrum of the 2,7-AQDS electrolyte after cycling (Fig. 6a). The present signals correspond to those before cycling (Fig. 6b). Consequently, the 2,7-AQDS electrolyte does not undergo any changes during charge/discharge and can be regarded as electrochemically stable. The ¹H-NMR spectra of the BQDS electrolytes differ significantly from each other. After 30 charge/discharge cycles, BQDS is still the main compound. The oxidized form of the BQDS is also present to a small extent, which is shown by the presence of the two singlets at 7.31 ppm (according to the

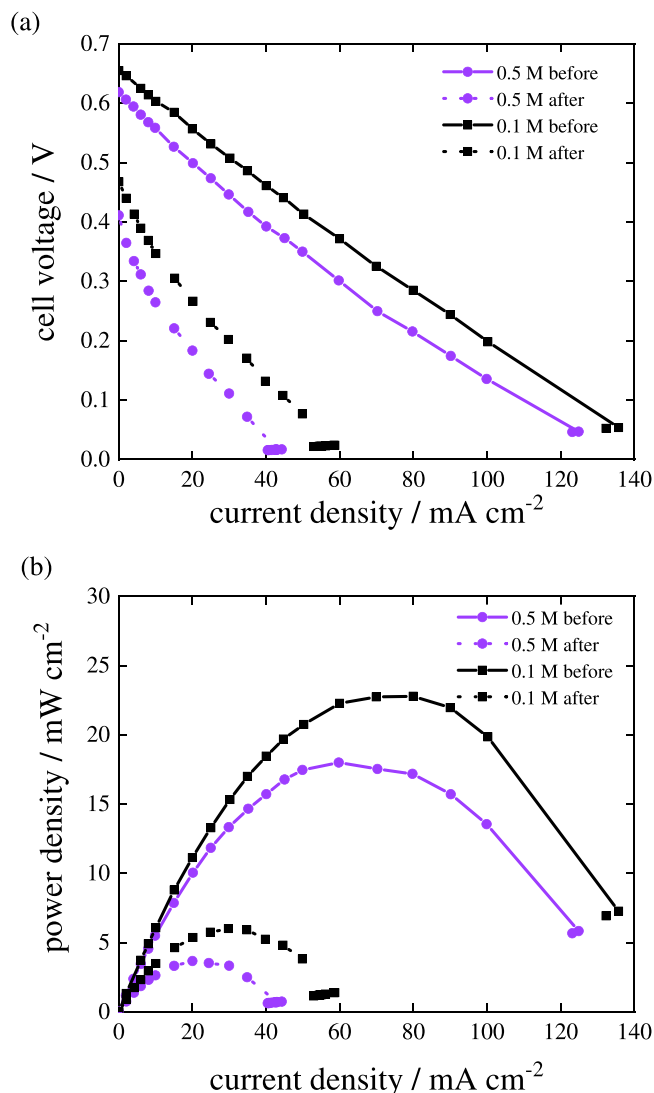


Figure 7. Polarization curves (a) and resulting power densities (b) for the flow cell with 0.1 M BQDS/2,7-AQDS (black) or 0.5 M BQDS/2,7-AQDS (purple) before (continuous line) and after (dashed line) charge/discharge studies.

proton in 6-position) and 7.62 ppm (according to the proton in 4-position), respectively. Another singlet occurs at 7.34 ppm. Due to the mere presence and the chemical shift of this signal it can be assumed that the newly formed compound is 1,2,4-trihydroxybenzene-3,5-disulfonic acid, since the 1,2,4,6-tetrahydroxybenzene-3,5-disulfonic acid has no aromatic proton. The occurrence of the Michael reaction, the structure of the corresponding Michael product, and the change in the BQDS electrolyte during the charge/discharge study can therefore be concluded from NMR spectroscopy. However, it is not possible to deduce the redox activity of this compound. This information can only be obtained using other analytical methods such as CV.

Furthermore, the ¹H-NMR spectra of the 2,7-AQDS and the BQDS electrolytes (Fig. 6c) do not comprise signals corresponding to the other electrolytes, which also confirms that no crossover has occurred.

The comparison of the polarization curve in Fig. 7a or the resulting power densities in Fig. 7b of the flow cell with BQDS/2,7-AQDS electrolytes before and after cycling clearly shows that the electrochemical instability of the BQDS has a negative effect on the performance of the entire cell. Already after 30 charge/discharge cycles, only 20% (0.5 M) respectively 26% (0.1 M) of the initial

maximal power densities can be achieved. Under these conditions, it is not possible to build a RFB only based on quinones comparable to VRFB.

It is also noticeable that with higher concentration of the active species the cell voltages and the resulting power densities decreases compared to the lower concentration. Since during the charge/discharge studies membranes and electrodes with similar properties are used, the main reason for the lower cell voltages and thus the higher ohmic resistance is a higher electrolyte resistance at higher concentrations of the active species. As we already emphasized, the conductivity of BQDS and 2,7-AQDS decreases while the viscosity especially of 2,7-AQDS increases with rising concentration of the active species. This also influences the electrolyte resistance and is probably the main reason for this increase.

Conclusions

In the present study we have carried out solubility, electric conductivity, viscosity as well as thermal and electrochemical stability studies of solutions with sulfuric acid as a solvent and quinones such as 2-AQS, 2,6-AQDS, 2,7-AQDS or BQDS as an organic active material.

Our results revealed that the solubility depends on the concentration of sulfuric acid (decrease with increasing concentration) and the temperature (20 °C < 40 °C). Likewise, the acids are much more soluble than the corresponding sodium salts. Furthermore, the solubilities of the considered quinones differ significantly from each other. Thus, the solubilities of 2-AQS and 2,6-AQDS are far too small for the realization of a competitive ORFB. However, the solubilities of 2,7-AQDS and BQDS in 1 M sulfuric acid are in the range of the vanadium solubility. The conductivity of solutions containing 2,7-AQDS or BQDS decreases with increasing concentration of active organic species, while the viscosity increases. The comparison with the vanadium electrolyte using 4 M sulfuric acid as supporting electrolyte shows that the conductivities of the quinone containing solutions are better for the same concentration of sulfuric acid and are comparable for 1 M sulfuric acid. The viscosity of the quinone containing solutions is even lower. By means of thermal treatment to test stability, it could also be shown that BQDS and 2,7-AQDS electrolytes are still stable at 40 °C after a storage period of 6 months. Due to these results, the use of 1 M sulfuric acid as a supporting electrolyte at 40 °C seems to be the best condition for building an appropriate ORFB.

We further analysed BQDS and 2,7-AQDS electrolytes after charge/discharge studies in a flow cell by using CV and NMR spectroscopy in order to consider the electrochemical stability. Both CV and NMR investigations show no changes in spectra of 2,7-AQDS electrolytes. This shows that crossover phenomena can be excluded and that this electrolyte can be considered electrochemically stable. In contrast to this, the BQDS spectra show signals of another compound, which is formed as a result of a Michael reaction and not by crossover. It could be proved that both methods give basically the same results in terms of (in)stability and crossover phenomena. However, each method also provides a deeper insight into properties that the other one cannot describe.

It also turned out that this electrochemical instability of the BQDS electrolyte leads to a considerable decrease of the cell performance. The lower cell voltage by using a higher concentration of active species also shows that the resistance of the electrolytes at high concentrations is higher than at lower concentrations, which is attributed to the decreasing conductivity.


Our study shows that quinone electrolytes must meet a whole range of requirements. These include sufficient solubility to achieve technically relevant values of the energy density, but also the highest possible electrical conductivity and low viscosity to keep the pumping losses and the resistance of the electrolyte as low as possible. The BQDS and the 2,7-AQDS electrolytes meet all these requirements. Unfortunately, despite good thermal stability, BQDS is not sufficiently stable under electrochemical stress, which has a

negative influence on the performance of the entire flow cell. Future work should therefore concentrate on the development of more stable molecules for the positive electrolyte, e.g. by chemical modification of BQDS.

Acknowledgments

This work was financially supported by Clausthal University of Technology, Germany.

ORCID

Stina Bauer  <https://orcid.org/0000-0002-7070-2804>
Dieter E. Kaufmann  <https://orcid.org/0000-0002-9790-828X>
Thomas Turek  <https://orcid.org/0000-0002-7415-1966>

References

- B. Dunn, H. Kamath, and J.-M. Tarascon, *Science (New York, N.Y.)*, **334**, 928 (2011).
- B. Zakeri and S. Syri, *Renewable Sustainable Energy Rev.*, **42**, 569 (2015).
- J. Winsberg, T. Hagemann, T. Janoschka, M. D. Hager, and U. S. Schubert, *Angew. Chem.*, **129**, 702 (2017).
- F. Pan and Q. Wang, *Molecules*, **20**, 20499 (2015).
- R. Ye, D. Henkensmeier, S. J. Yoon, Z. Huang, D. K. Kim, Z. Chang, S. Kim, and R. Chen, *J. Electrochem. En. Conv. Stor.*, **15**, 10801 (2018).
- B. Li and J. Liu, *Nat. Sci. Rev.*, **4**, 91 (2017).
- M. Park, J. Ryu, W. Wang, and J. Cho, *Nat. Rev. Mater.*, **2**, 16080 (2016).
- Y. A. Gandomi, D. S. Aaron, J. R. Houser, M. C. Daugherty, J. T. Clement, A. M. Pezeshki, T. Y. Ertugrul, D. P. Moseley, and M. M. Mench, *J. Electrochem. Soc.*, **165**, A970 (2018).
- L. F. Arenas, C. Ponce de León, and F. C. Walsh, *J. Energy Storage*, **11**, 119 (2017).
- M. Rychcik and M. Skyllas-Kazacos, *J. Power Sources*, **22**, 59 (1988).
- M. Skyllas-Kazacos, *J. Electrochem. Soc.*, **133**, 1057 (1986).
- K. Likit-anurak, K. Uthaichana, K. Punyawudho, and Y. Khunatorn, *Energy Procedia*, **118**, 54 (2017).
- M. Skyllas-Kazacos, *Encyclopedia of Electrochemical Power Sources* (Elsevier, Amsterdam) p. 444 (2009).
- C. Minke and M. A. Dorantes Ledesma, *J. Energy Storage*, **21**, 571 (2019).
- U.S. Geological Survey, *Mineral Commodity Summaries* (U.S. Geological Survey, Reston, United States of America) p.204 (2019).
- B. Huskinson, M. P. Marshak, C. Suh, S. Er, M. R. Gerhardt, C. J. Galvin, X. Chen, A. Aspuru-Guzik, R. G. Gordon, and M. J. Aziz, *Nature*, **505**, 195 (2014).
- P. Leung, A. A. Shah, L. Sanz, C. Flox, J. R. Morante, Q. Xu, M. R. Mohamed, C. Ponce de León, and F. C. Walsh, *J. Power Sources*, **360**, 243 (2017).
- V. Singh, S. Kim, J. Kang, and H. R. Byon, *Nano Res.*, **12**, 1988 (2019).
- Y. Ding, Y. Li, and G. Yu, *Chem.*, **1**, 790 (2016).
- S. Er, C. Suh, M. P. Marshak, and A. Aspuru-Guzik, *Chem. Sci.*, **6**, 885 (2015).
- J. E. Bachman, L. A. Curtiss, and R. S. Assary, *J. Phys. Chem. A*, **118**, 8852 (2014).
- C. Batchelor-McAuley, Q. Li, S. M. Dapin, and R. G. Compton, *J. Phys. Chem. B*, **114**, 4094 (2010).
- M. Quan, D. Sanchez, M. F. Wasylkiw, and D. K. Smith, *J. Am. Chem. Soc.*, **129**, 12847 (2007).
- A. Khataee, K. Wedege, E. Dražević, and A. Bientien, *J. Mater. Chem. A*, **5**, 21875 (2017).
- M. R. Gerhardt, L. Tong, R. Gómez-Bombarelli, Q. Chen, M. P. Marshak, C. J. Galvin, A. Aspuru-Guzik, R. G. Gordon, and M. J. Aziz, *Adv. Energy Mater.*, **7**, 1601488 (2017).
- W. Lee, A. Permatasari, B. W. Kwon, and Y. Kwon, *Chem. Eng. J.*, **358**, 1438 (2019).
- A. Khataee, E. Dražević, J. Catalano, and A. Bientien, *J. Electrochem. Soc.*, **165**, A3918 (2018).
- B. Hu, J. Luo, M. Hu, B. Yuan, and T. L. Liu, *Angew. Chem.*, **58**, 16629 (2019).
- Y. Ji, M. -A. Goulet, D. A. Pollack, D. G. Kwabi, S. Jin, D. Porcellinis, E. F. Kerr, R. G. Gordon, and M. J. Aziz, *Adv. Energy Mater.*, **9**, 1900039 (2019).
- Z. Yang, L. Tong, D. P. Tabor, E. S. Beh, M.-A. Goulet, D. de Porcellinis, A. Aspuru-Guzik, R. G. Gordon, and M. J. Aziz, *Adv. Energy Mater.*, **8**, 1702056 (2018).
- M.-A. Goulet and M. J. Aziz, *J. Electrochem. Soc.*, **165**, A1466 (2018).
- J. D. Hofmann, F. L. Pfanschilling, N. Krawczyk, P. Geigle, L. Hong, S. Schmalisch, H. A. Wegner, D. Mollenhauer, J. Janek, and D. Schröder, *Chem. Mater.*, **30**, 762 (2018).
- K. Lin et al., *Science*, **349**, 1529 (2015).
- D. G. Kwabi et al., *Joule*, **2**, 1894 (2018).
- W. Lee, A. Permatasari, and Y. Kwon, *J. Mater. Chem. C*, **8**, 5727 (2020).
- W. Lee, G. Park, and Y. Kwon, *Chem. Eng. J.*, **386**, 123985 (2020).
- A. W. Lantz, S. A. Shavali, W. Schroeder, and P. G. Rasmussen, *ACS Appl. Energy Mater.*, **2**, 7893 (2019).
- O. A. Ibrahim, P. Alday, N. Sabaté, J. P. Esquivel, and E. Kjeang, *J. Electrochem. Soc.*, **164**, A2448 (2017).
- L. Hooper-Burkhardt, S. Krishnamoorthy, B. Yang, A. Murali, A. Nirmalchandar, G. K. S. Prakash, and S. R. Narayanan, *J. Electrochem. Soc.*, **164**, A600 (2017).
- B. Yang, L. Hooper-Burkhardt, F. Wang, G. K. Surya Prakash, and S. R. Narayanan, *J. Electrochem. Soc.*, **161**, A1371 (2014).
- B. Yang, L. Hooper-Burkhardt, S. Krishnamoorthy, A. Murali, G. K. S. Prakash, and S. R. Narayanan, *J. Electrochem. Soc.*, **163**, A1442 (2016).
- A. Murali, A. Nirmalchandar, S. Krishnamoorthy, L. Hooper-Burkhardt, B. Yang, G. Soloveichik, G. K. S. Prakash, and S. R. Narayanan, *J. Electrochem. Soc.*, **165**, A1193 (2018).
- S. Zhang, X. Li, and D. Chu, *Electrochim. Acta*, **190**, 737 (2016).
- A. Permatasari, W. Lee, and Y. Kwon, *Chem. Eng. J.*, **383**, 123085 (2020).
- M. Kazacos, M. Cheng, and M. Skyllas-Kazacos, *J. Appl. Electrochem.*, **20**, 463 (1990).
- N. Kausar, R. Howe, and M. Skyllas-Kazacos, *J. Appl. Electrochem.*, **31**, 1327 (2001).
- M. Vijayakumar, L. Li, G. Graff, J. Liu, H. Zhang, Z. Yang, and J. Z. Hu, *J. Power Sources*, **196**, 3669 (2011).
- F. Rahman and M. Skyllas-Kazacos, *J. Power Sources*, **72**, 105 (1998).
- F. Rahman and M. Skyllas-Kazacos, *J. Power Sources*, **189**, 1212 (2009).
- M. Skyllas-Kazacos, *J. Electrochem. Soc.*, **143**, L86 (1996).
- H. E. Darling, *J. Chem. Eng. Data*, **9**, 421 (1964).
- M. Skyllas-Kazacos, L. Cao, M. Kazacos, N. Kausar, and A. Mousa, *Chem. Sus. Chem.*, **9**, 1521 (2016).
- Y. Xu, Y. H. Wen, J. Cheng, G. P. Cao, and Y. S. Yang, *AMR*, **396–398**, 1730 (2011).
- K. Wedege, E. Dražević, D. Konya, and A. Bientien, *Sci. Rep.*, **6**, 39101 (2016).
- Y. Xu, Y.-H. Wen, J. Cheng, G.-P. Cao, and Y.-S. Yang, *Electrochim. Acta*, **55**, 715 (2010).